ELSEVIER

Simulation of long-range transport of air pollutants over Northeast Asia using a comprehensive acid deposition model

Il-Soo Park[a],*, Won-Jun Choi[b], Tae-Young Lee[b], Suk-Jo Lee[a], Jin-Seok Han[a], Cheol-Hee Kim[c]

[a]*Air Quality Research Department, National Institute of Environmental Research, Kyongseo-dong, Seo-gu, Incheon 404-170, South Korea*
[b]*Department of Atmospheric Sciences, Yonsei University, Seoul 120-749, South Korea*
[c]*Department of Atmospheric Sciences, Pusan National University, Busan 609-735, South Korea*

Abstract

A comprehensive acid deposition modeling system (CADM) was developed to simulate the long-range transport of air pollutants and regional acidic deposition processes over Northeast Asia. The main objective of the CADM is to facilitate efficient assessment by providing explicit information on long-range transboundary processes. The implemented modeling system in CADM is composed of a numerical atmospheric model (CSU RAMS) and an Eulerian chemistry/transport/deposition model.

For the model validation, CADM was used to simulate long-range transport over the Northeast Asian region during 5–12 March 2002, and the simulated concentrations were compared with both surface observations at background monitoring stations as well as aircraft measurements. Additional experiments were performed to examine the sensitivity of simulated concentrations to input fields (emission rate and meteorological fields). The simulated concentrations showed some encouraging agreements with some success for the temporal variation of surface SO_2 concentrations in comparison with both the observation at background monitoring stations and aircraft observation. However, disagreements were significant for NO_x and O_3 concentrations, showing large inconsistencies especially at higher levels. The magnitudes of this disagreement were found to have some dependence on both input fields of emission rate and meteorology.

© 2005 Elsevier Ltd. All rights reserved.

Keywords: Long-range transport; Comprehensive transport/chemistry model; Observed concentrations; Verification; Sensitivity to inputs

1. Introduction

The acidic deposition processes across neighboring countries have been one of the serious environmental problems in Northeast Asia over the past two decades.

The vigorous industrialization of Korea and China over the two decades resulted in significant deterioration of the air quality and eco-environment in China and neighboring countries. In some mega-cities in southern China, annual mean pH values in the order of 3 have been reported, which have not been experienced much by human beings, while the minimum annual mean pH values in Europe and North America have been reported as being around 4.1 (Terada et al., 2002). Although there

*Corresponding author. Tel.: +82 32 560 7370; fax: +82 32 568 2040.

E-mail address: nierpis@me.go.kr (I.-S. Park).

are relatively fewer studies on the acidic deposition problem across national boundaries, there have been several studies on how SO_2 emitted in China affects ambient concentration and wet/dry deposition of SO_2 in Korea (Park and Cho, 1998). However, intense study of nitrogen deposition over Eastern Asia has not been conducted yet due to the complexities posed by its chemical reaction and the various nitrogen species involved in the deposition.

Model results for long-range transport and deposition may contain large errors, due to the uncertainties associated model (numerical treatment, physics and chemistry, etc.), emission rates, meteorological inputs, etc (e.g., Kotamarthi and Carmichael, 1990). These uncertainties may also result in large variability of predicted air quality, dry/wet deposition and source–receptor relationship. For example, the source–receptor relationship derived by a numerical model significantly varies with study (Huang et al., 1995; Ichikawa and Fujita, 1995). The model inter-comparison study by Carmichael et al. (2002), with identical inputs for meteorology and emission rates, has also shown that the numerically derived source–receptor relationship can vary greatly with model.

Improvement of a comprehensive modeling system requires the reduction of uncertainties associated with model, emission rates and meteorological inputs. Adequate verification is also an essential element of the improvement. Recently, several groups have produced useful data sets for verification of simulated long-range transport and deposition of air pollutants (e.g., Park et al., 2004; Okita et al., 1996). Adequate verification can reveal problems of modeling systems including input fields and direction of improvement.

This paper introduces a comprehensive modeling system, the comprehensive acid deposition model (CADM), which has been developed through cooperative research in Korea. It also presents the verification of CADM against the surface observations at background monitoring stations and aircraft observations, both of which clearly show long-range transports of air pollutants.

2. Components of comprehensive atmospheric model CADM

A CADM (Lee et al., 1998) has been developed by cooperative efforts of National Institute of Environmental Research and Yonsei University in Korea for prediction of air quality and deposition of air pollutants. The CADM can be operated in either on-line or off-line manner. The main part of CADM is composed of a regional-scale atmospheric model CSU RAMS (Pielke et al., 1992) and a chemistry/transport model developed by Lee et al. (1998). The descriptions of the model, input

data, and experimental design are briefly provided herein.

The conservation equation for the multiphase atmospheric transport/chemistry/deposition process in CADM can be written in the following form:

$$\frac{\partial C_i}{\partial t} = -\nabla \cdot (C_i \vec{V}) + \nabla \cdot (K_c \cdot \nabla C_i) + R_i$$
$$+ E_i + \left(\frac{\partial C_i}{\partial t}\right)_{\text{cloud}} + \left(\frac{\partial C_i}{\partial t}\right)_{\text{dry}}, \qquad (1)$$

where C_i is the concentration of the ith component, $\vec{V}$ the three-dimensional wind vector, K_c the eddy diffusion coefficient for the atmospheric pollutants, R_i the chemical transformation rate, E_i the rate of concentration change due to emission, and $(\partial C_i/\partial t)_{\text{cloud}}$ and $(\partial C_i/\partial t)_{\text{dry}}$ are the rates of concentration change due to cloud effects and dry deposition, respectively. The vertical eddy diffusion coefficient K_c was obtained from the profile functions of Brost et al. (1988). The present model employs the chemistry model of RADM to treat both the gas- (Stockwell et al., 1990) and aqueous-phase chemistry (Walcek and Taylor, 1986). The RADM considers 157 gaseous chemical reactions including 21 photochemical reactions involving 64 chemical species. Aqueous-phase chemistry considers 17 reactions for 9 components. Dry deposition is treated using the method of RADM (Chang et al., 1987). The details of the model can be found in Lee et al. (1998). The framework of the transport model for CADM is the same as the Yonsei University-Sulfur Acid Deposition Model (YU-SADM) (Lee et al., 1998), which considers sulfur only and uses a simple model for chemical transformation. YU-SADM is one of the participating models in the model inter-comparison study for transport and deposition in East Asia (MICS-Asia) (Carmichael et al., 2002).

## 3. Experimental design and observation data

This section presents the simulations of an episode for the spring season from 5 to 12 March 2002 and its comparisons with both aircraft measurements and surface observations at four background monitoring stations. Aircraft observations were carried out over the Yellow Sea on 7–9 and 11 March 2002.

3.1. Experimental design

The model domain covers eastern Asia, including Korea, eastern China, and Japan as illustrated in Fig. 1. The horizontal grid size is 60 km and the domain includes 68×56 grid points in horizontal plane. Vertical grids are composed of 28 vertical levels, vertically stretching with a stretch ratio of 1.15. The depth of the lowest vertical grid is 100 m.
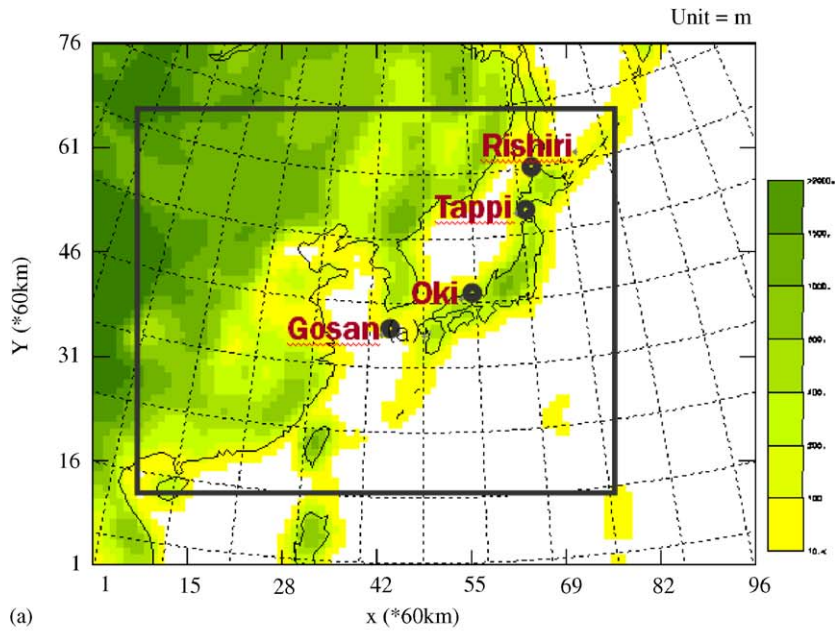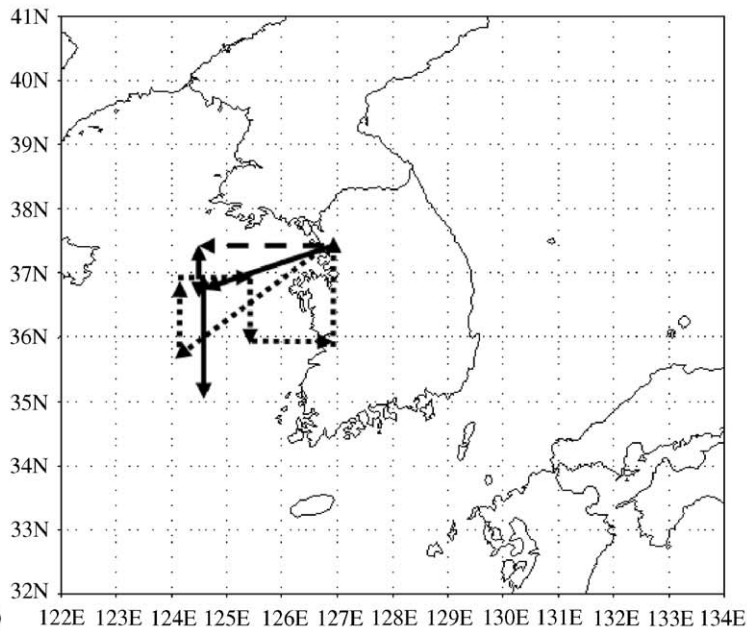
Fig. 1. The CADM domain and location of observation sites (a) and aircraft observation path made in March 2002 (b).

Model integrations were carried out over the model domain starting at 00 UTC 26 February with zero initial and boundary concentrations for all pollutants except

ozone (40 ppb) and terminate at 00 UTC 12 March 2002. The actual analysis was made for the period of 5–12 March, and thus the first 7 days prior to this analysis can

be regarded as the time for spin-up process over the model domain.

3.2. Inputs for CADM

In this study, CADM was operated in off-line manner. All of the required meteorological data such as winds (m/s), pressure (hPa), temperature (K), water vapor mixing ratio (kg kg^{-1}), accumulated amount (mm) of sub-grid scale explicit precipitation, surface temperature (K), mixing ratios (kg kg^{-1}) for cloud droplets including pristine ice, rain, snow, ice, and graupel were obtained from one hourly outputs of CSU RAMS (version 4.4) (Pielke et al., 1992). Six hourly GDAS data of NCEP in $1° \times 1°$ are used to provide initial and boundary conditions for the meteorological simulations. Simulation starts from 00 UTC 26 February through 00 UTC 12 March 2002, and four-dimensional data assimilation (FDDA) by Newtonian relaxation (nudging) is employed for the meteorological simulation.

Two emission data sets of SO_x and NO_x are employed to assess the impact of emission of a different emission inventory: first data set is completed through the Long-range Transboundary Air Pollutants in Northeast Asia (LTP) project (Choi et al., 2001), and the second one is from Streets et al. (2002). These data sets are used to obtain the emission rates of SO_x and NO_x on the $60 km \times 60 km$ CADM grids (Fig. 2). Emission rates for CO, NH_3 and anthropogenic NMVOC are from Streets et al. (2002). For natural VOC emission rate, Global Emission Inventory Activity (GEIA) (refer to http://groundhog.sprl.umich.edu/geia) data with a resolution of $1° \times 1°$ for the reference year of 1990 is used. Volcanic emissions are not considered in this study.

The detailed land-use type in each grid area obtained from the EPA/NOAA global ecosystem data was used for the precise calculation of dry deposition in which the land-use type is classified into 72 categories with 10′ latitude and longitude resolution. Since CADM considers 11 categories of land-use types, the EPA/NOAA land-use data over the model grids were regrouped for the corresponding categories of CADM.

3.3. Monitoring: aircraft measurement and surface monitoring

The aircraft observations were carried out over the Yellow Sea on 7–9 and 11 March 2002 in order to investigate in detail the concentrations of long-range transboundary pollutants. A total of three flight legs were carried out below 3 km above sea level (Fig. 1). The sampling domain was in the area of 124.3–128.0 E and 33.1–38.0 N. Each flight took 2.5–4.5 h and has flown above the mixed layer height. Upper air meteorological observation was also conducted during the aircraft test period over the western coastal area in Korea.

For the surface observations, a total of 4 stations are used for the validation of the model: Gosan (Jeju Island, Korea), Oki, Rishiri and Tappi (Japan) (Fig. 1). The details of surface and aircraft observations were well documented in the Annual Report of the LTP project for the year 2003 (Park et al., 2004).

3.4. Numerical experiments

Three experiments have been carried out to examine the dependence of simulations on both input fields of emission rate and meteorology. Experiment CON is intended for control run, which uses emission data of Streets et al. (2002) and strong nudging for FDDA in meteorological simulation using RAMS (nudging time scale of 3600 s). EXP1 uses emission rates from the LTP project (Choi et al., 2001) and EXP2 is the same as CON, except for a weak nudging (nudging time scale of 14,400 s). EXP1 is intended to assess the effect of different emission data sets, while EXP2 is to see the effects of varying meteorological inputs on the simulated concentration fields by applying significantly different strengths of nudging for meteorological simulation.

4. Results

4.1. Simulated meteorological fields

Fig. 2 shows the simulated sea-level pressure/wind fields and simulated daily precipitations during 7–11 March 2002. The simulated meteorological fields exhibit good agreement with the observed synoptic weather patterns for sea-level pressure and upper level fields (not shown). For example, sea-level pressure fields with relatively strong southwesterlies from southeastern China through the northern part of the Korean peninsula are well simulated for 00 UTC 9 March 2002 (Fig. 2). This field can induce a significant transport of air pollutants from China to the Korean peninsula. However, the simulated winds at other times are generally weak over eastern China and the Yellow Sea (Fig. 2).

According to the daily precipitation amount by the GPCP (Global Precipitation Climatology Project), significant precipitation does not appear over most of the continent and the Korean Peninsula. However, heavy rainfalls can be found over the Pacific Ocean and northern Japan during 7–10 March, and over southeastern China on 11, 12 March. The model simulation of rainfall amount is also found to be consistent with the observation in the fact that model has reproduced the rainfall around northern Japan and the Pacific Ocean on 7 March, and no rainfall was simulated over most of the domain on 8 and 9 March. Some of the rainfall in southern China was also simulated on 11 March (Fig. 2).

MSLP & Wind fields 00UT C 07 March   Simulated daily prec. 00UT C 07 March

MSLP & Wind fields 00UT C 09 March   Simulated daily prec . 00UTC 10 March

MSLP & Wind fields 00UT C 11 March   Simulated daily prec . 00UTC 11 March
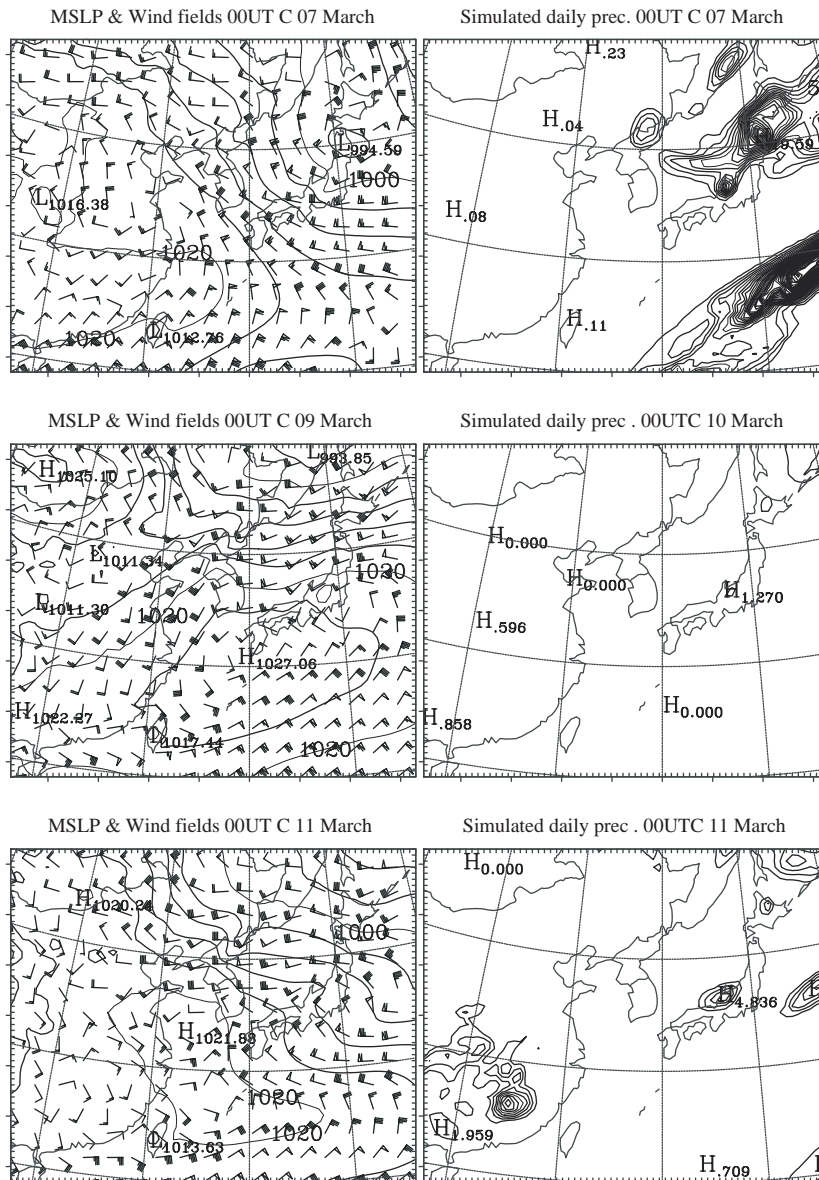

Fig. 2. Simulated sea-level pressure and wind fields (left panels) at 00 UTC for 7, 9 and 11 March 2002, and simulated daily precipitation amount for the previous 24 h (right panels) at 00 UTC for 7, 10 and 11 March 2002. The wind barb flag, staff and half staff represent 10, 2 and $1\,\mathrm{ms}^{-1}$, respectively. The precipitation amount contour starts from 1 mm with a 1 mm interval.

However, rainfall around northern Japan of 10 March is not simulated. These simulated results indicated that, overall, simulation of precipitation seems satisfactory considering the difficulty of predicting precipitation.

4.2. Simulated concentration fields

In order to substantiate the characteristics of the long-range transport process, two periods are selected: 5–6 March 2002 (Fig. 3) and 8–10 March 2002 (Fig. 4).

Later, verification of model results against observation will also be discussed for these periods. Simulated surface SO_2 concentration is shown in Fig. 3 for the first period (12 UTC 5–06 UTC 6 March 2002) and in Fig. 4 for the second period (18 UTC 8–00 UTC 10 March 2002) in 6 h intervals. The surface concentration over the emission area shows strong diurnal variation: relatively larger values at 18 UTC and smaller values at 06 UTC. As shown in Fig. 3, relatively higher concentrations are simulated over eastern China with
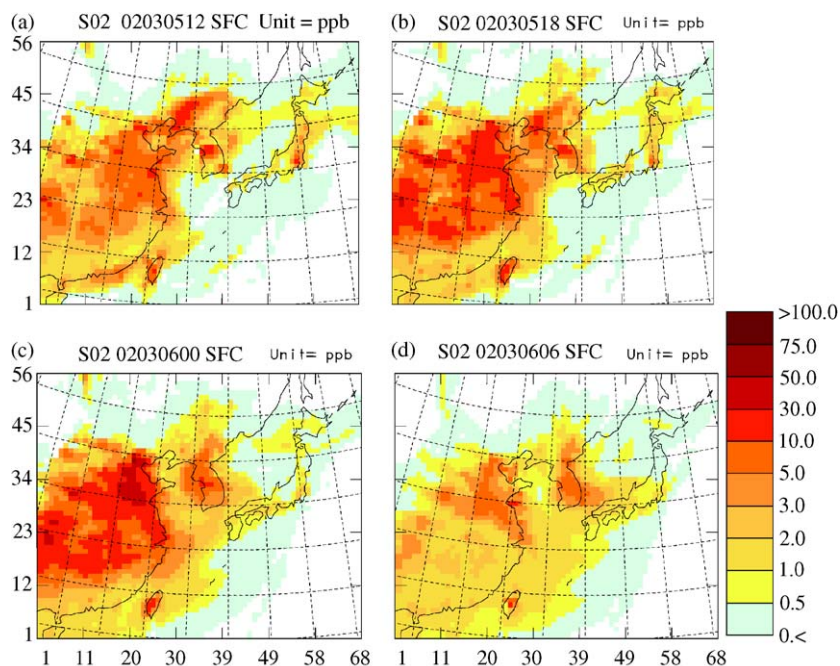
Fig. 3. Surface SO$_2$ concentration at (a) 12 UTC 5, (b) 18 UTC 5, (c) 00 UTC 6 and (d) 06 UTC 6 March 2002.

values exceeding 20 ppb at 00 UTC 6 March, indicating dominant southeastward transport of SO$_2$ by north-westerly over the whole Northeast Asia. As a result, considerably higher concentrations with a maximum SO$_2$ concentration of 20 ppb, which is much higher than normal background values (e.g., less than 1 ppb), are simulated over the Yellow Sea including the Korean peninsula and Jeju Island.

During the second period (8–10 March), long-range transport SO$_2$ from the source region of Eastern China toward northern Japan has occurred (Fig. 4). At 00 UTC 9 March, higher concentrations are simulated over the sea near Oki Island (Fig. 4b), showing relatively longer transport in comparison with the first case. According to the meteorological and concentration fields, these higher SO$_2$ concentrations might be attributed to the prevailing westerlies as depicted in Fig. 2. The long-range transport process associated with northern Japan (Rishiri) is also of interest, showing two predominant transports during this period. The first transport is found at 12 UTC 9 March across the sea between the Korean peninsula and northern Japan. A significant portion of this transport appears due to direct transport from the Korean peninsula by westerly. The second transport, which seems to be more complicated than the first case, occurs around 00 UTC 10 March. SO$_2$ emitted in Eastern China first moves northward on 7, 8 March and then veers a few degrees to north-eastward, thereby reaching the area to the north and northwest of the Korean peninsula at around 00 UTC 9

March. It then moves steadily southeastward, and reaches the area near Rishiri at around 00 UTC 10 March.

The NO$_2$ concentrations emitted from the Korean peninsula on 7, 8 March have also been transported eastward and reach northern Japan on 9 March (not shown). Although the transport of NO$_2$ is similar to that for SO$_2$, the transport from the Korean peninsula appears to be more pronounced compared with those transported from eastern China as described for SO$_2$.

4.3. Comparison of model results against surface observations

Temporal variations of simulated and observed surface SO$_2$ concentrations from 5 to 12 March 2002 are shown in Fig. 5. The comparisons are made for 4 background monitoring stations: Gosan (Jeju Island, Korea), Oki (Japan), Rishiri (Japan), Tappi (Japan). Locations of the station are indicated in Fig. 1. The simulated concentrations were in general agreement with the observations, showing the background level during the whole period except for the limited periods of long-range transport as described in Section 4.2.

Significant transport of SO$_2$ is detected at Gosan with the observed peak concentration of about 9 ppb at around 03 LST 6 March (Fig. 5a). The model has successfully reproduced this transport on 6 March, although the simulated peak values are relatively smaller than the observation. The increased concentration for
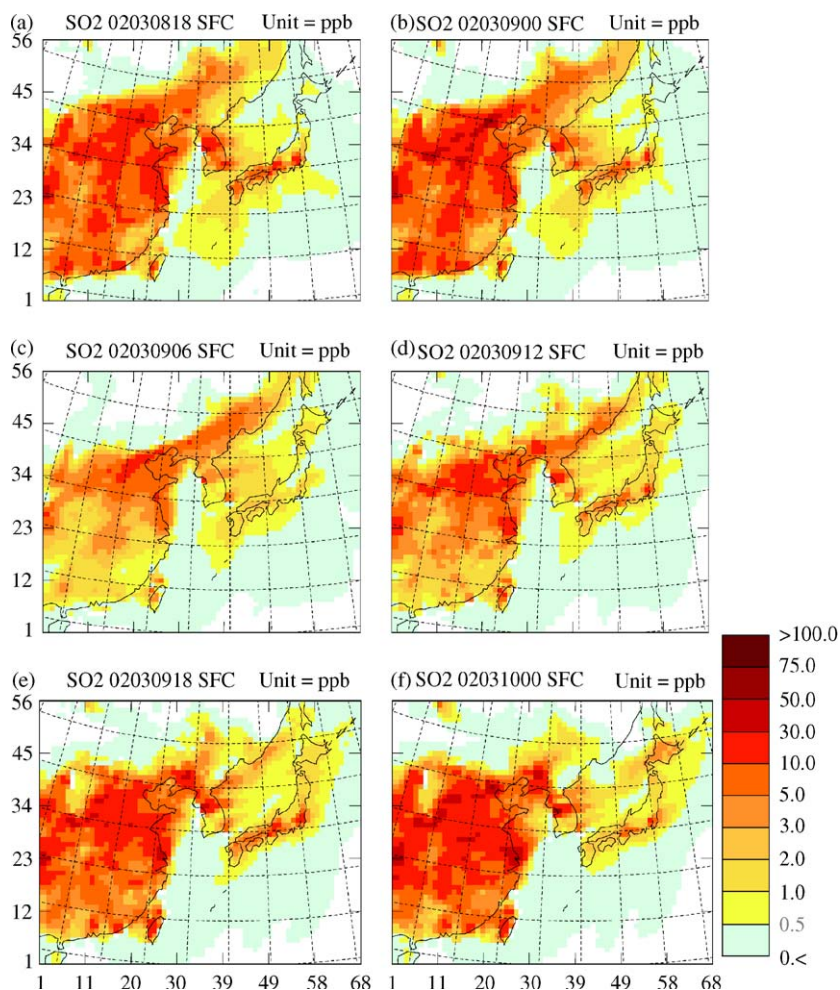
Fig. 4. Surface SO$_2$ concentration at (a) 18 UTC 8, (b) 00 UTC 9, (c) 06 UTC 9, (d) 12 UTC 9, (e) 18 UTC 9 and (f) 00 UTC 10 March 2002.

7–8 March at Gosan has also been simulated. The simulation has also successfully captured the major transport that occurred on 8–10 March at the three Japanese stations. Some inconsistencies are also found. For example, compared to observation, the simulation has produced several additional peak concentrations at Oki, which are likely to be due to false long-range transports. This inconsistency seems mainly associated with the incorrect simulation of mesoscale meteorological fields and precipitation, which can wash out pollutants before reaching the station.

The present results show that CADM predicts the long-range transport fairly well, given proper meteorological inputs. Some significant discrepancies are found between the experiments for the three Japanese stations. EXP2, which uses the same emission as CON but different meteorological input, shows a large difference from the other two experiments in the time and strength of peak concentrations for some occasions (e.g., 6, 7

March at Oki, 9, 10 March at Rishiri, and 6, 7 March at Tappi). CON and EXP1, which use identical meteorological input but different emission data, produce more significant overprediction at Tappi for 9, 10 March than EXP2. Note that at Tappi and Rishiri, which are further away from the major source areas, the impact of meteorological input appears more significant than that of emission.

The result of NO$_2$ shows that simulated concentrations over the whole period are generally smaller than the observation. Among the experiments, the experiment CON produces a relatively higher concentration of NO$_2$ in general than EXP1 during major transport periods, indicating the possibility that the emission rate of NO$_x$ may be the major source of uncertainties in this simulation. Ozone simulation also reveals some significant discrepancies between simulation and observation. At Gosan, simulated values are found to be significantly smaller than observation. Significant discrepancy is also
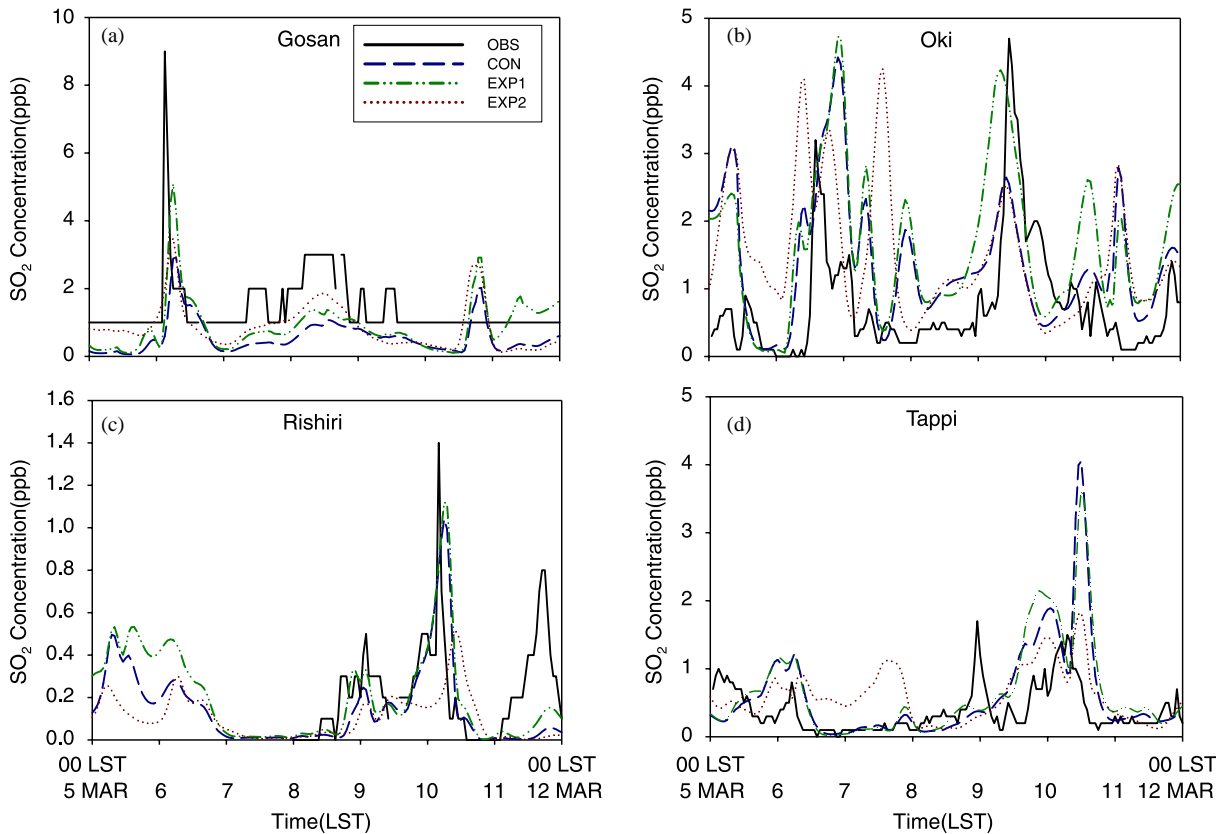
Fig. 5. Diurnal variation of SO$_2$ during the period of 5–12 March 2002 at monitoring stations in the area of background concentration level: (a) Gosan (Jeju Island, Korea), (b) Oki Islands (Japan), (c) Rishiri (Japan) and (d) Tappi (Japan) (CON and EXPs 1 and 2). Time is Korean time (UTC + 9 h).

Table 1
Simulated and observed daily mean surface concentrations for SO$_2$, NO$_x$* and O$_3$ (unit: ppb)

	Date	SO$_2$				NO$_x$*				O$_3$			
		CON	EXP1	EXP2	OBS	CON	EXP1	EXP2	OBS	CON	EXP1	EXP2	OBS
Gosan	06 March	1.15	1.61	1.29	1.91	0.63	0.54	0.47	3.67	38.76	37.06	43.48	44.54
	08 March	0.86	1.17	1.47	2.39	0.83	0.76	0.77	4.46	35.56	33.62	48.56	54.54
Oki	06 March	2.23	2.35	2.50	0.94	3.26	1.16	2.79	N/A	44.48	48.42	47.16	45.50
	09 March	1.50	2.53	1.47	2.03	6.02	2.64	4.88	N/A	40.91	44.15	38.28	62.00
Rishiri	09 March	0.20	0.22	0.16	0.30	1.12	0.28	0.80	0.85	24.78	28.66	27.04	56.05
	10 March	0.31	0.36	0.22	0.20	0.51	0.25	0.28	1.65	37.45	39.38	38.07	48.46
Tappi	09 March	1.00	1.15	0.86	0.46	3.15	1.06	2.72	1.52	30.80	36.62	26.96	59.92
	10 March	1.57	1.61	0.98	0.68	1.78	0.80	1.42	1.74	49.81	52.07	46.64	60.33

For Gosan, NO$_x$* includes only NO$_2$.

found at Rishiri, but at Tappi, simulation is relatively closer to observation (not shown).

The simulated daily mean surface concentrations are compared with observation for the period of long-range transports described in Section 4.2 (Table 1). Simulated SO$_2$ values are comparable to observations, except for

Oki on 6 March and Tappi on 9 March. The EXP1 experiment (use of LTP emission results) produces relatively more reasonable SO$_2$ concentration levels compared with the other 2 experiments, implying better simulation using the emission data established by the LTP project. The difference in nudging strength of

meteorological fields also produces some significant differences in simulated values; strong nudging shows smaller anomalies, which could explain the observation.

Simulated NO_2 concentrations are significantly smaller than observation for Gosan and Rishiri, while comparable at Tappi. EXP1, which uses LTP emission, shows especially smaller NO_2 concentrations than CON, which uses emission data of Streets et al. (2002), suggesting the necessity for improvement of source inventories.

4.4. Verification of model results against aircraft observation

Aircraft measurements were conducted for the validation of simulating the vertical structure of long-range transport over Northeast Asia. Although the aircraft observations are made over the limited area along the indicated flight paths as illustrated in Fig. 1, the results can suggest how the model reproduces some important features such as high concentration at higher levels as well as vertical locations of moving pollutants.

Table 2 shows the summary of comparisons between simulation and aircraft observations. The observed values are the averaged concentrations over the paths at a given height. The time and height of aircraft observations are also indicated in Table 2. The aircraft observation in general indicates that SO_2 and NO_x concentrations are significantly higher than background levels during the aircraft observation. For example, SO_2 concentration is found to be much higher than the background value especially in the layer above 500 m (on 7 March) and in the layer below 2000 m (on 8 March). Simulated values of SO_2 concentration agree fairly well with the aircraft observations in general. Simulation has captured the relatively large concentrations at high-levels (e.g., 2000 m) for 7 March, as well as below 2000 m for 8 March, although the magnitudes differ. The vertical variation of SO_2 concentration for 11 March is also very well simulated. Effects of varying input can be found in Table 2. Results from the three experiments often differ from each other significantly. Either EXP1 or EXP2 has produced SO_2 concentrations that are closer to the observation than CON. Consistency of simulation with the observation varies with the day. EXP2 fails to produce the relatively large concentration at 2000 m for 7 March, while it is most successful in simulating the vertical distribution for 11 March.

Observed NO_x concentrations are significantly larger than background level for most of the aircraft observations. This suggests both the existence of significant transport of pollutant at higher levels and the importance of the long-range transport process over Northeast Asia. However, the simulated NO_x concentrations are overall found to be fairly smaller than observations. Only EXP2 produces comparable simulations for 11 March, but higher NO_x concentrations at high-levels are not reproduced at all. In consideration of SO_2 concentration, these discrepancies are suggestive of reasons other than the transport process. Observed O_3 concentrations do not agree well with simulated concentrations

Table 2
Comparison with aircraft observations (unit: ppb)

Date	Height (m)	SO₂				NOₓ				O₃			
		CON	EXP1	EXP2	OBS	CON	EXP1	EXP2	OBS	CON	EXP1	EXP2	OBS
7 March	300	0.23	0.22	0.44	0.47	0.24	0.18	0.62	1.07	24.77	24.27	26.16	40.00
	500	0.19	0.19	0.39	1.90	0.16	0.13	0.42	2.14	24.16	23.56	26.50	41.20
	1000	0.18	0.24	0.47	1.41	0.16	0.08	0.33	2.01	27.94	27.15	35.18	40.70
	2000	1.39	2.02	0.29	3.32	0.85	0.39	0.16	3.01	74.31	74.65	71.42	39.45
	3000	0.45	0.17	0.14	2.44	0.07	0.04	0.05	2.49	62.04	61.34	59.96	40.25
8 March	500	1.74	2.59	6.81	2.08	0.24	0.22	3.38	4.25	54.60	51.60	69.32	24.65
	1000	8.48	8.25	7.88	2.97	1.16	0.34	4.99	7.97	119.70	110.32	71.56	26.35
	1500	5.06	8.58	0.47	3.31	1.89	1.57	0.23	8.15	75.57	77.96	36.58	25.30
	2000	0.56	1.06	0.19	1.26	0.23	0.30	0.14	6.30	36.48	36.94	39.82	23.05
	2500	0.01	0.02	0.39	0.57	0.01	0.04	0.20	4.29	28.72	29.14	39.83	20.60
9 March	700	1.96	2.78	3.54	3.21	0.33	0.26	0.97	5.69	53.4	47.4	55.3	58.9
	800	1.05	1.60	1.89	2.19	0.25	0.35	0.48	3.92	44.4	41.0	44.3	62.1
11 March	300	2.45	6.13	4.82	5.78	1.71	2.14	4.53	3.33	34.5	35.2	35.6	54.00
	500	1.51	3.55	3.12	3.80	0.78	0.87	2.65	3.11	31.9	32.6	33.3	54.10
	1000	1.24	1.51	1.82	1.81	1.03	0.48	1.02	2.21	25.2	27.4	39.3	46.70
	1500	1.11	1.52	0.57	0.42	0.97	0.38	0.33	1.13	35.8	37.8	50.7	40.50
	2000	0.24	0.38	0.12	0.10	0.18	0.15	0.22	1.26	39.4	39.5	50.5	39.30
	2500	0.36	0.06	0.05	0.03	0.04	0.10	0.11	1.07	36.7	37.7	47.1	36.00

with height, showing large discrepancies on 7 and 8 March except for 9 and 11 March.

Contrary to the successful reproduction of SO_2 concentration at both surface and aircraft-flight levels, we found larger discrepancies for NO_x and O_3 concentration. Although the plausible reasons for these discrepancies are not understood yet, more successful simulations might be hampered because of several factors such as incomplete emission inventory and difficulties in constructing appropriate boundary conditions.

The concentrations of SO_2 and O_3 at higher levels obtained by aircraft measurement in this study were found to be similar to that obtained during the TRACE-P experiment described by Carmichael et al. (2003). However, especially at higher levels, our modeling results show large inconsistencies from the aircraft observations for NO_x and O_3 concentrations. Thus, a thorough examination of the present modeling system is necessary to explain these inconsistencies in order to provide direction for model improvement.

5. Conclusion

This paper introduced the components of CADM, and described the CADM simulation of long-range transport processes over Northeast Asia during 5–12 March 2002. The simulated concentrations were compared with both surface observations at background monitoring stations and aircraft measurements.

Comparison of the simulated concentrations with observation showed some encouraging agreements: for example, CADM reproduced the temporal variation of surface SO_2 concentrations at background monitoring stations with some success, and the simulations were also consistent with aircraft observations to some extent. However, disagreements were significant for NO_x and O_3 concentrations, showing inconsistencies at both surface and higher levels. The magnitudes of disagreement showed some dependence on input fields of emission rate and meteorology. Therefore, further study is necessary for improving the present modeling system and reducing the uncertainties of emission inventory.

It is noted that the conclusions presented here were based on the comprehensive acid deposition model for several days only. Further studies considering many more episodes with extensive observations would be necessary to understand the complex long-range transport over Northeast Asia and to improve the modeling system. Presently, continued efforts are being made for both intensive monitoring and further comprehensive modeling in order to achieve model improvement through scientific cooperation between northeastern Asian countries.

References

Brost, R.A., Haagenson, P.L., Kuo, Y.-H., 1988. The effects of diffusion on tracer puffs simulated by a regional scale Eulerian model. Journal of Geophysical Research 93 (D3), 2389–2404.

Carmichael, G.R., Calori, G., Hayami, H., Uno, I., Cho, S.Y., Engardt, M., Kim, S.-B., Ichikawa, Y., Ikeda, Y., Woo, J.H., Ueda, H., Amann, M., 2002. The MICS-Asia study: model intercomparison of long-range transport and sulfur deposition in East Asia. Atmospheric Environment 36, 175–199.

Carmichael, G.R., Tang, Y., Kurata, G., Uno, I., Street, D., Woo, J.-H., Huang, H., Yienger, J., Lefer, B., Shetter, R., Blake, D., Altas, E., Fried, A., Apel, E., Eisele, F., Cantrell, C., Avery, M., Barrick, J., Sachse, G., Brune, W., Sandholm, S., Kondo, Y., Singh, H., Talbot, R., Bandy, A., Thorton, D., Clarke, A., Heikes, B., 2003. Regional-scale chemical transport modeling in support of the analysis of observations obtained during the TRACE-P experiment. Journal of Geophysical Research 108 (D21), 8823.

Chang, J.S., 1987. Development and implementation of chemical mechanism for the regional acid deposition model (RADM), technical notes. National Center for Atmospheric Research, Boulder, Colorado 242pp.

Choi, K.-D., Kim, J.-S., Kim, B.G. (Eds.), 2001. Annual Report for the 1st year's Joint Research on Long-Range Transboundary Air Pollutants in Northeast Asia. Secretariat of Working Group for LTP Project, 2001, NIER, Korea, 121pp.

Huang, M., Wang, Z., He, D., Xu, H., Zhou, L., 1995. Modeling studies on sulfur deposition and transport in East Asia. Water, Air, and Soil Pollution 85, 1927–1932.

Ichikawa, Y., Fujita, S., 1995. An analysis of wet deposition of sulfate using a trajectory model for East Asia. Water, Air, and Soil Pollution 85, 1921–1926.

Kotamarthi, V.R., Carmichael, G.R., 1990. The long range transport of pollutants in the pacific rim region. Atmospheric Environment 24A, 1521–1534.

Lee, T.-Y., Kim, S.-B., Lee, S.-M., Park, S.-U., Kim, D.-S., Shin, H.-C., 1998. Numerical Simulation of air quality and acid deposition for episodic cases in eastern Asia. Korean Journal of the Atmospheric Sciences 1 (2), 126–144.

Okita, T., Hara, H., Fukuzaki, N., 1996. Measurements of atmospheric SO_2 and SO_4^{-2}, and determination of the wet scavenging coefficient of sulfate aerosols for the winter monsoon season over the Sea of Japan. Atmospheric Environment 30, 3733–3739.

Park, J.W., Cho, S.Y., 1998. A long range transport of SO_2 and sulfate between Korea and east China. Atmospheric Environment 32 (16), 2745–2756.

Park, I.-S., Kim, J.-C., Lee, D.-W. (Eds.), 2004. Annual Report for the 4th year's Joint Research on Long-range Transboundary Air pollutants in Northeast Asia. Secretariat of Working Group for LTP Project, 2004, NIER, Korea, 392pp.

Pielke, R.A., Cotton, W.R., Walko, R.L., Tremback, C.J., Nicholls, M.E., Moran, M.D., Wesley, D.A., Lee, T.J., Copeland, J.H., 1992. A comprehensive meteorological modeling system—RAMS. Meteorology and Atmospheric Physics. 49, 69–91.

Stockwell, W.R., Middleton, P., Chang, J.S., Tang, X., 1990. The second generation regional acid deposition model chemical mechanism for regional air quality modeling. Journal of Geophysical Research 95, 16343–16367.

Streets, D.G., Bond, T.C., Carmichael, G.R., Fernandes, S., Fu, Q., He, D., Klimont, Z., Nelson, S.M., Tsai, N.Y., Wang, M.Q., Woo, J.-H., Yarber, K.F., 2002. A year-2000 inventory of gaseous and primary aerosol emissions i n Asia to support TRACE-P modeling and analysis.

Journal of Geophysical Research special TRACE-P issue.

Terada, H., Ueda, H., Wang, Z., 2002. Trend of acid rain and neutralization by yellow sand in east Asia-a numerical study. Atmospheric Environment 36, 503–509.

Walcek, C.J., Taylor, G.R., 1986. A theoretical method for computing vertical distributions of acidity and sulfate production within cumulus clouds. Journal of the Atmospheric Sciences 43, 339–355.